**DEUTSCHES ELEKTRONEN-SYNCHROTRON DESY**

DESY SR-79/24
October 1979



# LASER INDUCED RECRYSTALLISATION AND DEFECTS IN ION IMPLANTED HEXAGONAL SiC

by

V. V. Makarov, T. Tuomi and K. Naukkarinen

*Laboratory of Physics, Helsinki University of Technology,*
*SF-02150 Espoo 15, Finland*

M. Luomajärvi and M. Riihonen

*Department of Physics, University of Helsinki,*
*SF-00170 Helsinki 17, Finland*

NOTKESTRASSE 85 · 2 HAMBURG 52

To be sure that your preprints are promptly included in the
HIGH ENERGY PHYSICS INDEX ,
send them to the following address ( if possible by air mail ) :

DESY
Bibliothek
Notkestrasse 85
2 Hamburg 52
Germany

DESY SR-79/24
October 1979

# LASER INDUCED RECRYSTALLISATION AND DEFECTS IN ION IMPLANTED HEXAGONAL SiC

V. V. Makarov[a)], T. Tuomi and K. Naukkarinen
Laboratory of Physics, Helsinki University of Technology,
SF-02150 Espoo 15, Finland

M. Luomajärvi and M. Riihonen
Department of Physics, University of Helsinki, SF-00170 Helsinki 17,
Finland

## ABSTRACT

SiC(6H) crystals amorphized with $^{14}N^{+}$-ion implantation were annealed with $CO_2$ laser pulses at intensities of 20 to 100 MW/cm$^2$. Laser produced crystallisation due to residual ray absorption was studied by means of optical spectroscopy, $^{4}He^{+}$-ion backscattering spectrometry and channeling as well as Cu $K_{\alpha 1}$ and synchrotron x-ray diffraction topography. At low laser intensities topographs revealed linear and planar defects which contributed to increased dechanneling independent of analyzing beam energy. Minimum of lattice disorder, which was in some regions of the laser impact area smaller than that obtained in thermal annealing, was attained at the peak laser intensities of about 50 MW/cm$^2$.

To appear in Appl. Phys. Letters.

---

a) on leave from M.I. Kalinin Leningrad Polytechnic Institute, USSR



It is known that thermal annealing of silicon carbide crystals does not result in complete removal of radiation damage even at as high a temperature as 1800°C, at which the crystal surface starts to decompose (1, 2). It is therefore of considerable interest to explore the possibilities of high intensity laser irradiation which has proved successful in the annealing of ion-implanted silicon (3, 5).

Fig. 1 shows the optical absorption spectrum of SiC(6H) single crystals (curve a) (6, 7) and that of SiC made amorphous by ion bombardment (curve b). Curve b was calculated from the optical density and reflectivity measured in this work using the value of the thickness of the amorphous layer obtained from the measured He-ion Rutherford backscattering (BS) spectra. It is seen that there is a large shift of the absorption edge towards lower photon energies when the crystal is made amorphous. Consequently, possible lasers for annealing amorphous SiC are Nd-, ruby or $N_2$-lasers, whose photon energies are 1.17 eV, 1.79 eV and 3.67 eV, respectively. However, a strong dependence of the absorption coefficient $\alpha$ on the degree of disorder should result in a dependence of the required laser intensity on the implantation conditions. In addition, a single $N_2$-laser light pulse of 5 ns duration would heat only a thin subsurface layer of some tens of a nm, because the absorption coefficient for this light is rather large ($\alpha > 3 \cdot 10^5$ cm$^{-1}$).

Another possibility is to use a $CO_2$-laser, because its photon energy (117 meV) is within the Reststrahlen (residual ray) band of lattice absorption. According to Ref. 8, $\alpha = 6 \cdot 10^3$ cm$^{-1}$ for amorphous SiC and

$\alpha = 1 \cdot 10^4\ cm^{-1}$ for crystalline SiC at this photon energy, i.e. the absorption does not depend significantly on the disorder. In this case the laser light intensity necessary for annealing should still depend on the degree of damage because of the different reflectivities of the amorphous and crystalline SiC (20% and 90%, respectively (8)). The results reported in this work were obtained using pulsed TEA $CO_2$ lasers, the pulse length of which was 0.1 μs. Also some experiments were made with pulsed Nd- and $N_2$ lasers and it was found that they probably can be used for annealing of SiC.

N-type SiC(6H) crystals, the net donor concentration of which was about $2 \cdot 10^8\ cm^{-3}$, were implanted at room temperature with 45 keV $^{14}N^+$-ions. The diameter of the overlapping $CO_2$-laser beam spots on the sample was from 0.3 to 1 mm. BS random and in the <0001>-direction aligned spectra of the etched as-grown, implanted and annealed parts of the SiC samples were taken with a 0.8 mm diameter $^4He^+$-ion beam of a van de Graaff accelerator. For further investigation of the annealed crystals x-ray diffraction topography using characteristic $CuK_\alpha$ radiation of an x-ray generator and synchrotron radiation of the DORIS electron-positron ring was applied (9). Optical measurements were performed with a curved grating monochromator using a Xe-lamp as a light source.

Figure 2 shows the random (a) and aligned (b to e) energy spectra of 1 MeV $^4He^+$ particles backscattered from the SiC crystal implanted with $8 \cdot 10^{15}\ {}^{14}N^+$ ions/cm$^2$. Curve b of Fig. 2 is the spectrum of the as-implanted part of the sample, curve c was obtained after irradiation with partially overlapping 1 mm-diameter laser pulses whose maximum intensity



in the center was about 20 MW/cm$^2$. The optical absorption spectrum of the same laser irradiated part of the crystal is shown in Fig. 1, curve c. The absorption coefficient is 10 to 20% of that of the amorphous material. Because of the simultaneous decrease of absorption coefficient and the thickness of the damaged layer, the optical transmittance of the laser annealed region at 3 eV is only about 10% less than that of the unimplanted region. Therefore by visual inspection it is difficult to distinguish between the laser annealed and the unimplanted regions of the crystal. The BS spectrum of Fig. 2 (curve c) shows, however, that there is a lot of damage left in the crystal. A striking feature of this spectrum is that the dechanneling level (observable in Fig. 2, curve c, at depths larger than 150 nm) is higher than in the as-implanted crystal (Fig. 2, curve b), although the damage peak near the surface is lower than that in the as-implanted crystal. This can be explained by the existence of large scale imperfections such as stacking faults, dislocations or twins. The analysis of the BS spectra taken at different He-ion beam energies (0.5 MeV, 1.0 MeV and 2.0 MeV) suggests that major contribution to the dechanneled component is due to defects, the dechanneling cross-section of which does not depend on the beam energy. According to Ref. 10, this is the case of stacking faults. Only about 1/7 of the dechanneling is caused by displaced atoms.

Figure 3 shows a {11 · 12} characteristic $CuK_{\alpha 1}$-radiation back reflection topograph and Fig. 3b a {01 · 1} white synchrotron radiation transmission topograph of the same 20 MW/cm$^2$-laser annealed crystal whose optical absorption and BS spectra were shown in Fig. 2 (curve c) and in Fig. 1 (curve c). In Fig. 3 unimplanted (I), implanted (II) and laser pulse irradiated (III) regions are seen. A dark line between areas I and II is due to lateral strain caused by the expansion of the implanted amorphous layer (II). Traces of the circular laser spots are seen in region III. Within each spot there are three systems of narrow ($\sim 1 \mu m$) straight lines (L) parallel to $\langle 11 \cdot 0 \rangle$. These lines are more clearly visible in Fig. 3c which is a larger magnification than in Fig. 3a and b from a part of region III. The lines may be interpreted as diffraction images of slip planes or stacking faults in agreement with the conclusion made from the analysis of the BS spectra. However, enough information from different reflections was not yet obtained to perform a complete fault vector analysis.

Circular lines (C) around the laser spots in Fig. 3a and b are most likely of the same origin as the boundary line between region I and II, i.e. they separate the crystalline (laser annealed) and the amorphous (as-implanted) regions. The transmission topograph (Fig. 3b) shows how the strain field extends outside the laser spot. Two short sections of the boundary line between regions I and II were hit by the laser beam. As seen from the topograph they did not, however, disappear indicating that complete restoration to the original state was not attained. In addition to the defects caused by ion implantation and laser irradiation, some curved long dislocations as well as stacking faults deep in the crystal are seen in Fig. 3b. Also the damage caused by the He-ion beam (A) is visible in the x-ray topographs (Fig. 3a, b and d).

Curve d of Fig. 2 shows the BS spectrum of SiC measured after irradiation with 50 $MW/cm^2$ laser pulses. Although the residual damage is considerably smaller than after 20 $MW/cm^2$ irradiation (curve b), the normalized yield behind the damage peak is about 10% which is still larger by a factor of



about 3 than that of the unimplanted crystal (curve f). An x-ray topograph of the 50 $MW/cm^2$ annealed crystal is shown in Fig. 3d. Only separate dark spots (S) in the middle of large annealed areas are seen. They are evidently due to damage in the center of the laser spots where the light intensity has its maximum.

When the laser light intensity is increased up to 100 $MW/cm^2$, the BS spectrum (Fig. 2, curve e) shows no damage peak near the surface. However, the dechanneling level is rather high. A similar phenomenon and a change in the Ga to As concentration ratio has been observed in laser damaged GaAs (12). In SiC, however, no noticeable change in the Si to C concentration ratio could be found. An x-ray reflection topograph (Fig. 3e) shows dark spots which are larger than those in Fig. 3d observed after 50 $MW/cm^2$ irradiation.

It is interesting to notice that the largest removal of damage by means of $CO_2$ laser pulses calculated in this work from the BS spectra (Fig. 2d) is very closely the same as that obtained by thermal annealing at 1700° C of 30 keV $n^+$-implanted SiC crystals (13). The analysing He-ion beam was larger in diameter than the distance between the small dark laser damaged spots in the x-ray topograph (Fig. 3d). Lower level of damage might have been observed in the BS spectrum, if the spots could have been excluded. This, in turn, means that laser annealing is probably more efficient than thermal annealing.

---

This work was supported by the Finnish Ministry of Education (V.V.M.), the Alexander von Humboldt-Stiftung (T.T.) and the Emil Aaltosen säätiö (K.N.).

References

1 V.V. Makarov, Fiz. Tverd. Tela., 13, 2357 (1971) (Sov. Phys. Solid State 13, 1974 (1972))

2 L. Patrick and W.J. Choyke, Phys. Rev. B 5, 3253 (1972)

3 I.B. Khaibullin, K.I. Shtyrkov, M.M. Zaripov, M.F. Galyautdinov and G.G. Zakirov, Sov. Phys.-Semicond. 11, 190 (1977) and references therein.

4 B.A. Kachurin, N.B. Pridachin, and L.S. Smirnov, Sov. Phys.-Semicond. 9, 946 (1975)

5 See e.g. Proceedings of "Laser effects in ion implanted semiconductors" Catania, August 31 - September 2, 1978, ed. by E. Rimini.

6 W.J. Choyke and L. Patrick, Phys. Rev. 172, 769 (1968)

7 V.V. Makarov, Fiz. i Tekhn. Poluprov. 6, 1805 (1972). (Soviet Physics - Semicond. 6, 1556 (1973))

8 E. A. Fagen, Silicon Carbide 1973, Proc. 3d Int. Conf. on SiC, Edts. R.C. Marshell, J.W. Faust Jr., C.E. Ryan, South Carolina Press, 1974, p. 542

9 T. Tuomi, K. Naukkarinen, E. Laurila and P. Rabe, Acta Polytecnica Scand. Ph 100, 1 (1973), phys. stat. sol. (a) 25, 93 (1974)

10 E. Rimini, p. 455 in Material Characterization Using Ion Beams, Ed. J.P. Thomas and A. Cachard, Plenum Press 1976.

11 M. Lefeld-Sosnowska and E. Zielińska-Rohozińska, phys. stat. sol. (a) 35, K1 (1976)



12 R. Tsu, J.E. Baglin, G.J. Lasher, and J.C. Tsang, Appl. Phys. Lett. 34 (2), 153 (1979).

13 A.B. Campbell, J.B. Mitchell, J. Shewchun, D.A. Thomson and J.A. Davies, Silicon Carbide 1973, Proc. 3d Int. Conf. on SiC, Edts. R.C. Marshall, J.W. Faust Jr., C.E. Ryan, South California Press, 1974, p. 486.

14 H.J. Leamy, G.A. Rozgonyi, T.T. Sheng and G.K. Celler, Appl. Phys. Lett. 32, 535 (1978) and references therein.

15 G.N. Maracas, G.L. Harris, C.A. Lee and R.A. McFarlane, Appl. Phys. Lett. 33, 453 (1978).

Captions of Figures

Fig. 1 Optical absorption spectrum of (a) monocrystalline SiC(6H), (b) ion-implanted amorphous and (c) 20 MW/cm$^2$ $CO_2$-laser annealed SiC.

Fig. 2 1 MeV $^4He^+$ backscattering spectra of SiC: (a) random and (b) <0001>-aligned incidence on $8 \cdot 10^{15}$ $^{14}N^+$ ions/cm$^2$ implanted sample. <0001>-aligned spectra were also taken after (c) 20 MW/cm$^2$, (d) 50 MW/cm$^2$, (e) 100 MW/cm$^2$ pulsed $CO_2$-laser annealing. (f) is the <0001>-aligned spectrum of the unimplanted crystal.

Fig. 3 (a) {11 · 12} reflection $CuK_{\alpha 1}$-topograph, (b) {01 · 1} synchrotron radiation transmission topograph of a SiC crystal showing unimplanted (I), implanted (II) and 20 MW/cm$^2$ laser annealed (III) regions. (c) Magnification of (a), region III. (d) {11 · 12} reflection $CuK_{\alpha 1}$-topograph of a 50 MW/cm$^2$ laser annealed SiC crystal and (e) that of a 100 MW/cm$^2$ laser annealed crystal. (Regularly spaced parallel straight lines in (e) are similar to those observed in Ref. 14, 15).

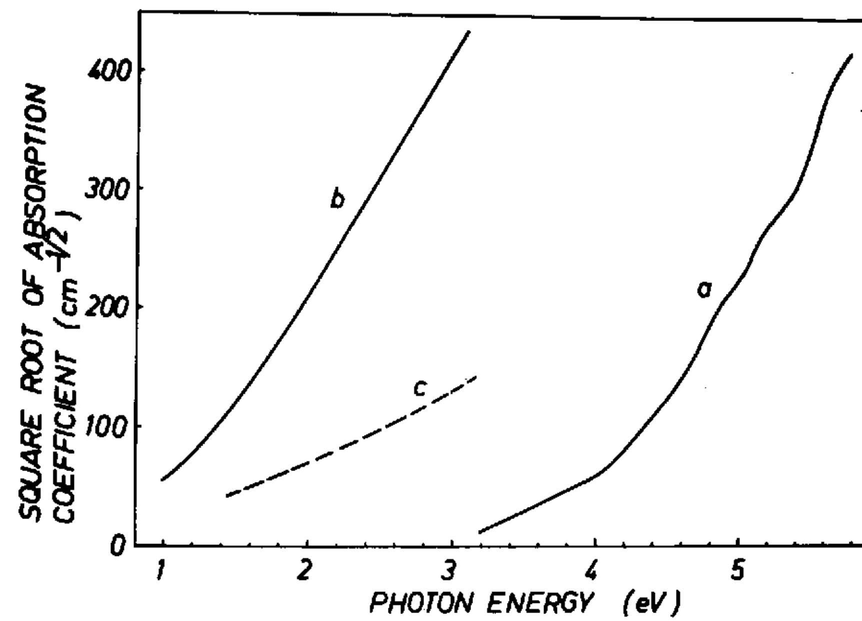


FIG.1

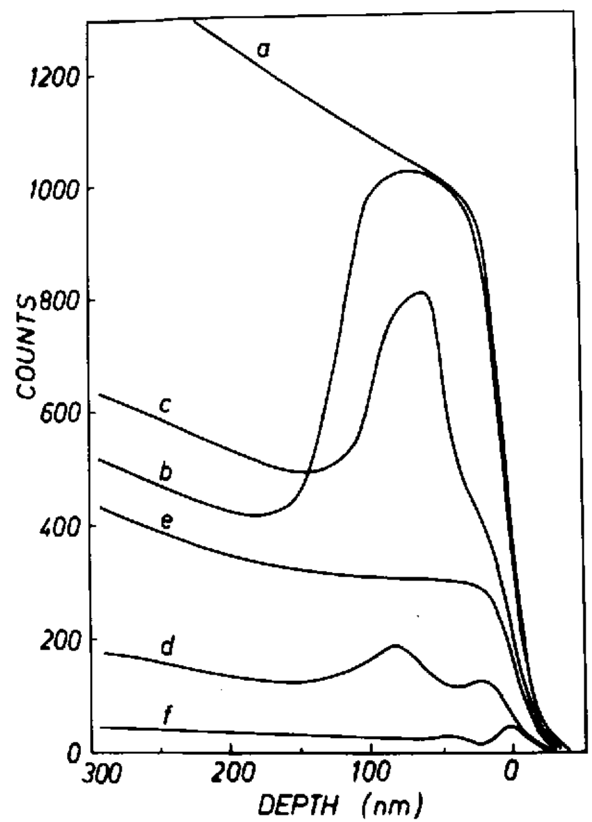

a
c
b
e
d
f
1200
1000
800
600
400
200
0
COUNTS
300
200
100
0
DEPTH (nm)


FIG.2

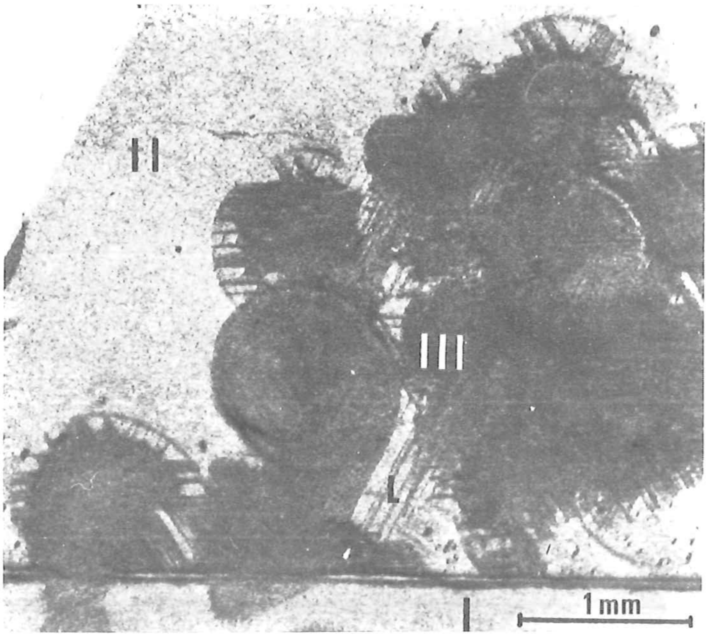


FIG.3a

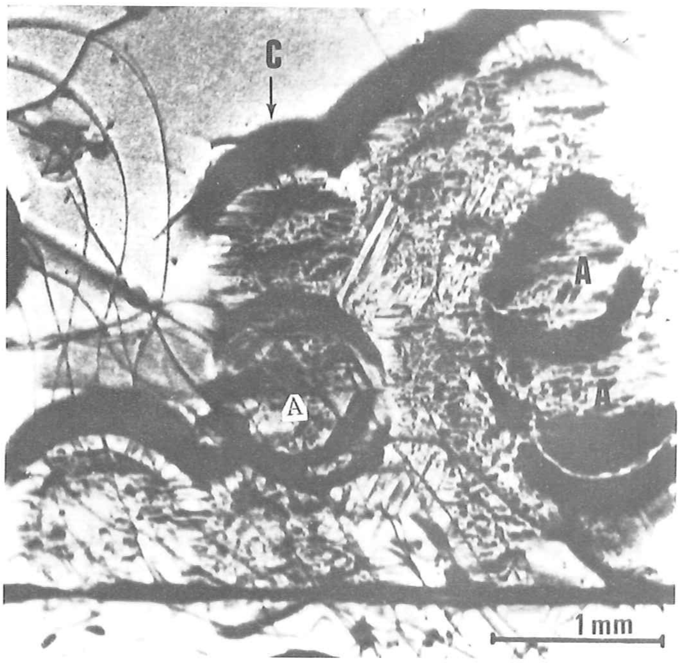


b

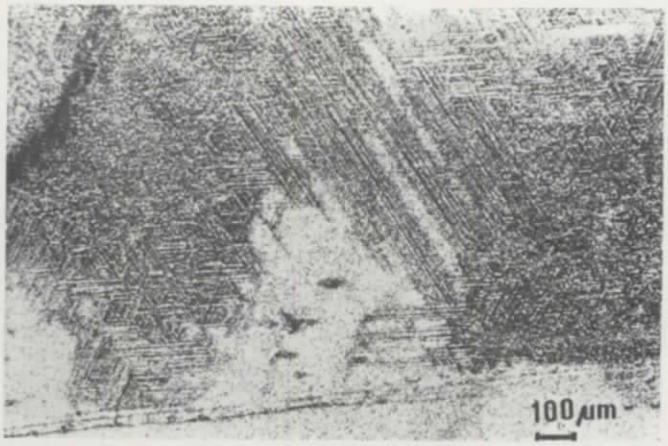


c

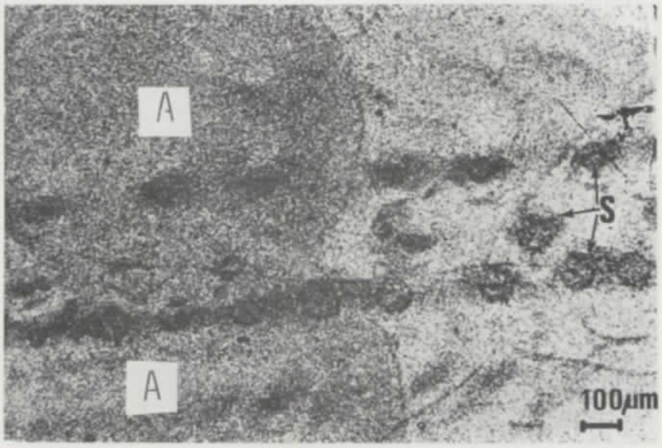


d

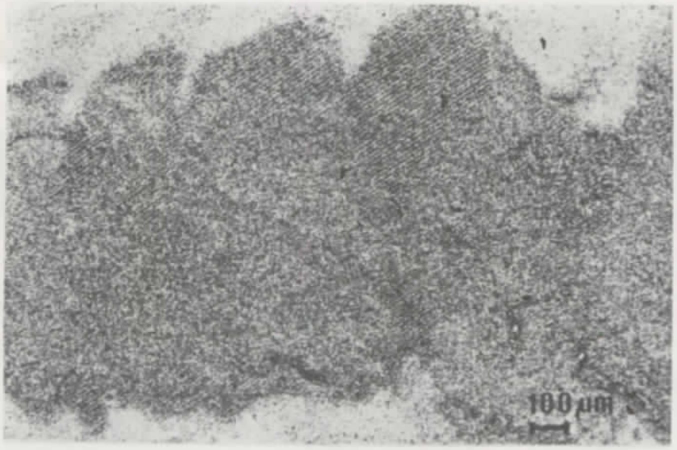


e